

Blockage of Water Flow in Carbon Nanotubes by Ions Due to Interactions between Cations and Aromatic Rings

Jian Liu,^{1,2} Guosheng Shi,^{1,*} Pan Guo,^{1,2} Jinrong Yang,^{1,2} and Haiping Fang^{1,†}

¹*Division of Interfacial Water and Key Laboratory of Interfacial Physics and Technology, Shanghai Institute of Applied Physics, Chinese Academy of Sciences, Shanghai 201800, China*

²*University of Chinese Academy of Sciences, Beijing 100049, China*

(Received 26 January 2015; revised manuscript received 27 July 2015; published 16 October 2015)

Combining classical molecular dynamics simulations and density functional theory calculations, we find that cations block water flow through narrow (6,6)-type carbon nanotubes (CNTs) because of interactions between cations and aromatic rings in CNTs. In wide CNTs, these interactions trap the cations in the interior of the CNT, inducing unexpected open or closed state switching of ion transfer under a strong electric field, which is consistent with experiments. These findings will help to develop new methods to facilitate water and ion transport across CNTs.

DOI: 10.1103/PhysRevLett.115.164502

PACS numbers: 47.61.-k, 31.15.xv, 61.48.De, 89.40.Cc

Understanding and controlling the behavior of water molecules across carbon-based nanochannels is of great importance. It has attracted widespread attention in water desalination and purification [1,2], nanofluidic manipulation [3–10], the design of biomimetic pores [11–13] based on carbon nanotubes (CNTs), precise molecular sieving through graphene or graphene-oxide membranes [14,15], and understanding biological activities in cellular transport phenomena [16–18]. In practice, the behavior of water molecules across carbon-based nanochannels is usually significantly affected by the ionic environment [14,19–24]. However, in recent years, some serious discrepancies have arisen between theory and experiments, which has greatly hindered the understanding of the properties and applications of carbon-based nanochannels. For example, it has long been expected that the narrow (6,6)-type CNT can be used as an excellent seawater desalination membrane [1,25,26] because of its experimentally confirmed ultrafast pure water flow [27–31] and theoretically predicted ion rejection [25,26,32–36]. However, to date, there is insufficient experimental evidence of adequate salt rejection for desalination [2], even though fabrication of CNT membranes has greatly improved [37–39].

As another example, in recent experiments in the design of human-made biological ion channels, Strano *et al.* observed unexpected ion pore-blocking behavior in wide (diameter > 1 nm) single-walled CNTs in salt solutions [22–24,40]. Because of the presence of cations (Li^+ , Na^+ , K^+ , and Cs^+), the CNTs exhibited special open or closed Coulter-state switching for current carried by protons when the system was above a threshold voltage. Otherwise, the channel maintains a closed state under lower voltages [22–24]. Unfortunately, this ion pore blocking and open or closed state switching of ion transfer cannot be explained using classical molecular dynamics (MD) simulations [40]; this is partly because the interactions between hydrated

cations and the CNT in classical MD simulations only contain van der Waals interactions, which are not sufficient to trap ions in the CNTs.

Most carbon-based nanochannel surfaces, such as CNTs, nanoporous graphene, graphene-oxide laminate, and aromatic rings in biomolecules and organic molecules, contain an aromatic structure, which is a hexagonal carbon ring rich in π electrons. Although there are only weak interactions between aromatic rings and water molecules, the aromatic rings strongly interact with cations, referred to as cation- π interactions [41]. However, in the study of the behavior of water molecules across carbon-based nanochannels, cation- π interactions are usually ignored, despite their important roles in various systems and applications, such as control of the structure and function of microscale and nanoscale materials, macromolecules, and proteins [21,41–48]. We recently investigated cation- π interactions between hydrated ions and carbon-based structures in aqueous solution, and our theoretical prediction of ion enrichment on graphite surfaces [49] was confirmed by the recent experiment of Joshi *et al.* [14]. Molecule-thick pancakes of aqueous NaCl solution on graphite surfaces, due to cation- π interactions between hydrated Na^+ in solution and surfaces predicted by theory, have also been experimentally observed [50]. Thus, cation- π interactions should be considered in the analysis and numerical simulations of the hydrated ion behavior inside or near CNTs.

Here, we show that these discrepancies between theory and experiments arise from a misunderstanding of the interaction of hydrated ions with CNTs. Combining classical MD simulations and density functional theory (DFT) calculations, we show that water flow in narrow (6,6)-type CNTs is blocked by cations in solution because of strong noncovalent cation- π interactions. By functionalizing the CNT entrance with saturated groups ($-\text{CH}_2\text{CH}_2-$) or applying an electric field along the

channel, this ion blocking can be prevented while maintaining a fast water flow rate (> 40% of that in the same system for pure water) through the CNT and 100% ion rejection. In the wider (8,8)-type CNT, our calculations show that Na^+ ions are easily trapped in the interior of the CNT, and an electric field above a threshold value will allow the cations to escape from the trapped state and move through the channel, inducing open or closed state switching of ion transfer. This has been observed in experiments, but has not been previously predicted by theoretical analysis or numerical simulation. Moreover, simulations with K^+ , $\text{N}(\text{CH}_3)_4^+$, and Cl^- are also consistent with experimental results. These findings provide new insight for the understanding and design of desalination membranes, new types of nanofluidic channels, nanosensors, and nanoreactors based on a CNT platform.

We first obtained the energy curve for adsorption of Na^+ ion to a 14-Å-long (6,6)-type CNT ($\text{C}_{144}\text{H}_{24}$) at the B3LYP/6-31G(d) level in the Gaussian-09 program [51]. The curve is relatively flat in the interior of the CNT and sharply increases at the two entrances [Fig. 1(a)]. A fitting curve constructed from two arctangent (arctan) functions was used to model the potential of Na^+ in the CNT,

$$E^{\text{cation}-\pi}(z) = \frac{\alpha\varepsilon}{\pi} \{ \arctan[\lambda(z - z_m)] + \arctan[\lambda(-z - z_m)] \}, \quad (1)$$

where z is the distance between Na^+ and the center of the CNT along the tube's z axis, ε is the adsorption energy of the Na^+ at the center of the CNT, and the parameters z_m , α , and λ are fitting coefficients. For the Na^+ with the (6,6)-type CNT, $\varepsilon = 29.5 \text{ kcal mol}^{-1}$. $\alpha = 1.1$ is a fitting coefficient from the adsorption energy obtained by quantum mechanical calculation, to be applied to the potential curve. $z_m = 8.6 \text{ \AA}$ and $\lambda = 1.6 \text{ \AA}^{-1}$ are parameters for adjusting the shape of the platform. The analysis of residual charges shows a clear amount of charge transfer between the adsorbed Na^+ and the CNT [see Fig. 1(b)]. Energy decomposition analysis and molecular orbital analysis show that the orbital interaction provides the main adsorption energy of Na^+ adsorbed in the CNT (see Supplemental Material PS1 [52]). We implemented the interactions between hydrated cations in solution and π -electron-rich aromatic rings in the CNTs in the parallel simulation program NAMD [62] based on the DFT calculations (see Supplemental Material PS2–6 [52]). The CHARMM Lennard-Jones (L-J) potentials remain; then, the total potential for Na^+ in CNT is $E^{\text{cation}-\pi} + E^{\text{L-J}}$, as shown in Fig. 1(a). All of the MD simulations were performed under periodic boundary conditions in the canonical (NVT) ensemble at 300 K (see Supplemental Material PS7 [52]).

We use hydrated Na^+ in the narrow (6,6)-type CNT as an example to illustrate the concept of water flow blocked by cations in solution. The simulation system consisted of a filter membrane formed by four (6,6)-type CNTs, as shown in Fig. 1(c). A NaCl solution with 500 water molecules and 10 NaCl pairs is on the left, and pure water is on the right. A pressure difference of 20 MPa was obtained between the two entrances of the CNT by applying a constant force on an impermeable wall [64].

Figure 1 clearly shows that water flow in these narrow CNTs is blocked by ions. In the 20-ns simulation, the first CNT channel is blocked by Na^+ at the entrance starting at 0.4 ns, and all of the channels are blocked by ions after 2.5 ns, as shown in Fig. 1(c). For comparison, we also performed MD simulations without cation- π interactions. In this case, the Na^+ ions were dispersed in the solution and all of the channels remained open.

The flow trajectories are shown in Fig. 1(d) (the first 15 ns is shown, and the full 20-ns trajectories are provided in Supplemental Material PS8 [52]). Water flow stopped at 2.5 ns when all of the channels were blocked by Na^+ . Interestingly, the flow rate was 3.0 ns^{-1} per nanochannel and slightly fluctuated in the process of Na^+ binding to the CNTs from 0.4 to 2.5 ns, shown by the pink shaded region in Fig. 1(d). This flow rate was much higher than that in the same system without cation- π interactions (1.2 ns^{-1} per nanochannel). We measured the number of

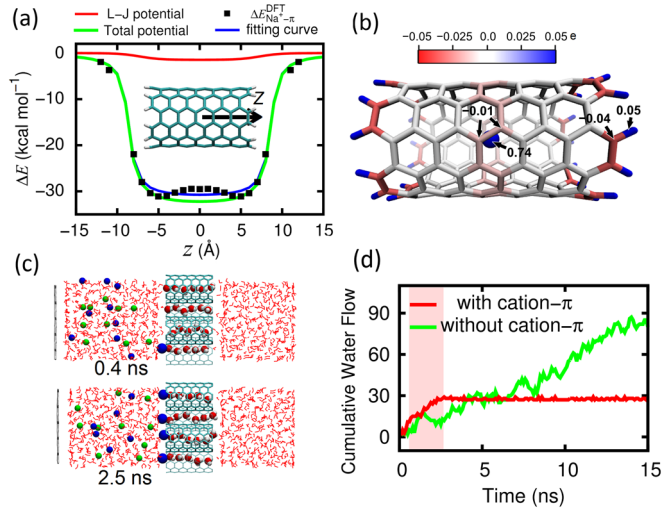


FIG. 1 (color online). (a) DFT adsorption energies (ΔE) between Na^+ and CNT (black squares); DFT potential (blue line) fitted from those adsorption energies; classical charmm L-J potential (red line); total potential (green line) by incorporating the DFT potential into the classical CHARMM L-J potential. z is the distance between Na^+ and the center of the CNT along the tube's z axis. (b) Residual Hirshfeld charge [63] distribution of Na^+ adsorbed in the center of a (6,6)-type CNT. (c) Snapshots of the modeling system, comprising a filter membrane (four CNTs) and two reservoirs with cation- π interactions. (d) Cumulative water flow through the CNT membrane with (red) and without (green) cation- π interactions. Na, Cl, O, and H atoms are shown as blue, green, red, and white spheres, respectively, and water molecules outside the tubes are shown as red lines. The time range of the binding process (0.4 to 2.5 ns) is highlighted by the shaded pink region.

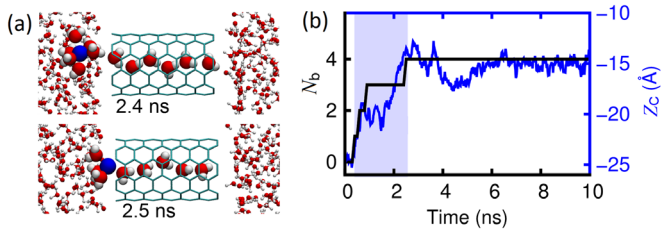


FIG. 2 (color online). (a) Na^+ position and structure of the water shell in the binding process. (b) Number of Na^+ ions bound at the entrance of the CNTs (N_b , black line), and the center of mass of Na^+ along the z direction (z_c , blue line) as a function of time. The time range of the binding process is highlighted by the blue shaded region.

Na^+ ions bound at the entrance of the CNTs (N_b) and the center of mass of all Na^+ (z_c) in the binding process. The Na^+ moved towards the CNT from 0.4 to 2.5 ns [blue shaded region in Fig. 2(b)]. During this Na^+ binding process, the water molecules traveled through the channel in the same direction, leading to significant water flow. Moreover, the structure of the first Na^+ hydration shell changed in the binding process. A typical case is shown in Fig. 2(a). During the first 2.4 ns, the Na^+ ions diffused in the solution with mainly six-coordinated water molecules in its first hydrated shell. After the Na^+ bound to the entrance of the CNT channel at 2.5 ns, the first hydrated shell around the bound Na^+ changed to four-coordinated water molecules. Three of these water molecules were located on the bulk side, and one was located in the interior of the CNT channel. The steric effect of the CNT confined the coordinated water molecules in a small space, leading to changes in the structure of the hydrated shell. Moreover, additional simulations of the other four parallel systems, H-terminated CNT, larger system, and longer simulation time also showed water blocking by Na^+ , indicating that the blocking of water flow in CNTs by ions generally occurs (Supplemental Material PS9–12 [52]).

It is clear that water flow can recover if instability can be created in the location of the cations at the binding sites. One idea is to functionalize the ends of the CNTs with saturated $-\text{CH}_2\text{CH}_2-$ groups (see Supplemental Material PS13 [52] for details) to attempt to prevent any direct contact of Na^+ with the aromatic rings of the CNT. The results of MD simulations with these functionalized CNTs are shown in Figs. 3 and S11. In the 20-ns simulations, the water flow rate reached 0.7 ns^{-1} per nanochannel, which is $\sim 40\%$ of the water flow in the same system with pure water (without any ions) of 1.7 ns^{-1} per nanochannel [see Fig. 3(a)]. Given that water moves from the solution to the pure water reservoir against an osmotic gradient of $\sim 6 \text{ MPa}$, the flow rate is still very high because the water permeability is enhanced by 2–3 orders of magnitude in the nanometer-sized CNTs [30]. Functionalization of the ends of the CNTs with $-\text{CH}_2\text{CH}_2-$ groups weakens the cation- π interaction between Na^+ and the CNTs, resulting

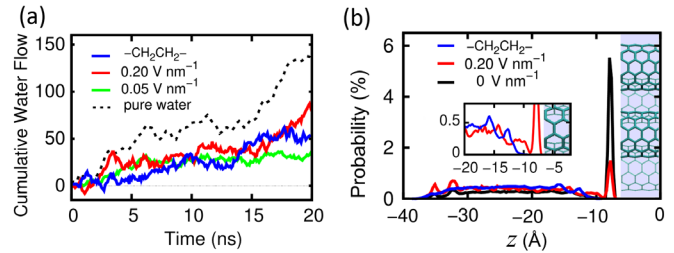


FIG. 3 (color online). (a) Cumulative water flow through the CNT driven by pressure as a function of simulation time in the system with (6,6)-type CNT tubes. Water flow for CNTs functionalized with $-\text{CH}_2\text{CH}_2-$ groups (blue line), the application of electric fields of 0.05 and 0.20 V nm^{-1} (green and red lines, respectively), and pure water (black dashed line) are shown. (b) Distribution probabilities of Na^+ in the NaCl solution along the z direction. The blue shaded region denotes the location of the CNT. For comparison, an additional system without applying an electric field or functionalizing the ends of the CNTs (black solid line) is also shown.

in an absence of bound Na^+ at the entrance [i.e., no peak in the distribution probability of Na^+ near the entrance in Fig. 3(b)].

We can also apply an electric field E along the channel from the pure water side to the salt solution side to pull the cations away from the binding site. The simulation results (Fig. 3, with more details in Supplemental Material PS14 [52]) indicate that an electric field exceeding 0.05 V nm^{-1} forced the channel to open. When the electric field exceeded 0.20 V nm^{-1} , the water flow rate reached 1.0 ns^{-1} per nanochannel, as shown in Fig. 3(a), which is about 60% of the flow of pure water through the CNT filter membrane. The distribution probability of Na^+ at the binding sites ($z = -7.8 \text{ \AA}$) significantly decreased under the electric field [see Fig. 3(b)]. That is, Na^+ could not stably bind to the entrance of CNT channel, and, thus, water flow recovered.

In (8,8)-type CNTs, Na^+ ions are trapped in the interior of the CNT under no electric field [Fig. 4(a)], and the trapped Na^+ may result in the experimentally observed ion pore-blocking behavior [22–24]. With application of a strong electric field (E), the Na^+ ions escape from the channel at 3 ns under $E = 0.25 \text{ V nm}^{-1}$, as shown in Fig. 4(b). Further increasing E causes additional Na^+ to escape from the channel [see Fig. 4(b)]. We found that there are four and five such cases for $E = 0.25$ and 0.30 V nm^{-1} , respectively. This indicates that under a strong electric field, the channel has a Coulter status. Thus, when there are no trapped ions, the complete hydrogen bond (HB) network is favorable for proton transfer (an open state). However, when a Na^+ ion is bound to the channel, the HB network would be partially broken by the Na^+ so that proton transfer is unfavorable (a closed state). Furthermore, the dwell time (τ), which is defined as the width of the closed state, decreased from 20 ns (from analysis of the full MD

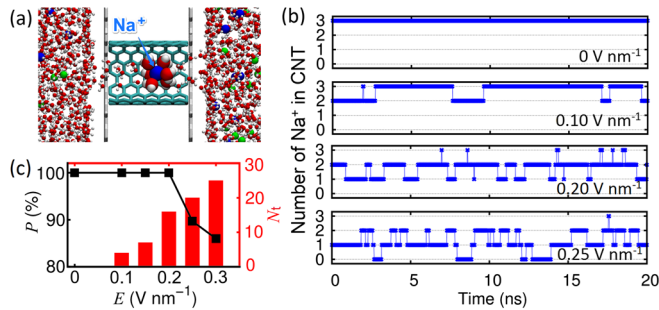


FIG. 4 (color online). Open or closed state switching of ion transfer in a (8,8)-type CNT by Na^+ . (a) Snapshots of the modeling system, comprising an (8,8)-type CNT and two solution reservoirs with cation- π interactions. The trapped Na^+ in the CNT channel is indicated by the arrow. (b) Number of Na^+ ions in the CNT as a function of time under various electric fields. (c) Na^+ trapping probability P and the number of transport Na^+ N_t through the CNT in the 20-ns simulation trajectories with respect to electric field E .

trajectories) for $\leq 0.20 \text{ V nm}^{-1}$ to 3.6 ns at 0.25 V nm^{-1} and 2.9 ns at 0.30 V nm^{-1} , and the trapping probability P also decreased with increasing electric field [see Fig. 4(c)]. These trends with electric field are consistent with experimental observations [22,23], but the dwell time in the simulation is much shorter than that in experiments (about 10 s). We should point out that the 500- μm -long CNT used in experiments is much longer than the 1.4-nm CNT used in the simulations, which may result in different dwell times. The ion mobility, which is defined as the proportionality factor of an ion's velocity and electric field, was $0.2 \times 10^{-8} \text{ m}^2 \text{ V}^{-1} \text{ s}^{-1}$ in the simulation system, which is close to the experimental value of $5 \times 10^{-8} \text{ m}^2 \text{ V}^{-1} \text{ s}^{-1}$ for Na^+ [22]. If the experimental CNT length is scaled from 500 μm to 1.4 nm with the ion mobility held constant, the dwell time would be about 0.1 ns, which is close to that obtained from the simulation.

The simulations without cation- π interactions show that Na^+ will not be trapped in the CNT, and, thus, the CNT remains in an open state (see Supplemental Material PS15 [52] for details).

Moreover, our calculations on the behaviors of K^+ , $\text{N}(\text{CH}_3)_4^+$, and Cl^- are also consistent with experimental results. K^+ shows open or closed state switching of ion transfer, and its ion transport rate is higher than that of Na^+ . $\text{N}(\text{CH}_3)_4^+$ does not show any trapping characteristics because its large $-\text{CH}_3$ groups will attenuate the interaction between the positively charged center N atom and the CNT by the steric effect, which considerably reduces the cation- π interactions. The interaction between the hydrated Cl^- anion and the CNT is very weak, which is similar to the interaction between the hydrated Cl^- anion and the graphite surface [49,65]. Consequently, Cl^- also does not result in pore blocking.

In summary, the strong noncovalent interactions between hydrated cations in solution and carbon-based π -electron-rich structures (cation- π interactions) were incorporated within classical MD simulations to study the behavior of the cations near and inside CNTs. For narrow (6,6)-type CNTs, we found that Na^+ easily bind at the entrance of the CNT, resulting in the blocking of water flow through the nanotube. In the (8,8)-type CNT, we found that the Na^+ ions are easily trapped in the interior of the CNT, and these trapped Na^+ ions can escape from the trapped state and move through the channel under an electric field above a threshold value. This explains the mechanism of unexpected open or closed state switching of ion transfer observed in experiments [22–24,40]. Simulations with K^+ , $\text{N}(\text{CH}_3)_4^+$, and Cl^- are also consistent with experimental results. For example, $\text{N}(\text{CH}_3)_4^+$ does not show any pore-blocking characteristics, because of the weak cation- π interaction and the large steric effect. We emphasize that the good agreement between our computational results and experimental observations further illustrates the importance of cation- π interactions in the study of the behavior of ion solutions with CNTs, and demonstrates the robustness and reliability of the calculations used in the present study.

Based on the understanding of the behavior of ions and water near and inside narrow (6,6)-type CNTs, we propose two methods to prevent the blocking of CNTs by ions while allowing ultrafast water flow with ion rejection: (1) functionalization of the ends of the CNTs with saturated groups ($-\text{CH}_2\text{CH}_2-$) to prevent any direct contact between Na^+ and the π -electron-rich aromatic rings of the CNT; (2) application of an electric field to pull the cations away from the inlets of the CNTs. We hope that these methods will be helpful for future development of efficient desalination membranes based on CNTs.

Our findings highlight the crucial role of cation- π interactions in the behavior of hydrated ions on typical hydrophobic aromatic-rich carbon-based materials, such as CNT and graphene, and provide insight into the applications of nanofluidic manipulation, extremely sensitive ion detection and separation at the single-molecule level, drug delivery, and biomimetic pore design.

We thank Dr. Rongzheng Wan, Dr. Yi Gao, Dr. Chunlei Wang, Dr. Beien Zhu, and Dr. Dongqi Wang for their constructive suggestions. This work was supported by the National Natural Science Foundation of China (Grants No. 11290164 and No. 11404361), the National Basic Research Program of China (973 Program Grant No. 2012CB932400), the Shanghai Natural Science Foundation of China (Grant No. 13ZR1447900), the Key Research Program of Chinese Academy of Sciences (Grant No. KJZD-EW-M03), the Deepcomp7000 and ScGrid of Supercomputing Center, the Computer Network Information Center of Chinese Academy of Sciences and the Shanghai Supercomputer Center of China.

- *shiguosheng@sinap.ac.cn
†fanghaiping@sinap.ac.cn
- [1] M. A. Shannon, P. W. Bohn, M. Elimelech, J. G. Georgiadis, B. J. Marinas, and A. M. Mayes, *Nature (London)* **452**, 301 (2008).
- [2] M. Elimelech and W. A. Phillip, *Science* **333**, 712 (2011).
- [3] R. Z. Wan, J. Y. Li, H. J. Lu, and H. P. Fang, *J. Am. Chem. Soc.* **127**, 7166 (2005).
- [4] J. Y. Li, X. J. Gong, H. J. Lu, D. Li, H. P. Fang, and R. H. Zhou, *Proc. Natl. Acad. Sci. U.S.A.* **104**, 3687 (2007).
- [5] X. J. Gong, J. Y. Li, H. Zhang, R. Z. Wan, H. J. Lu, S. Wang, and H. P. Fang, *Phys. Rev. Lett.* **101**, 257801 (2008).
- [6] L. Bocquet and E. Charlaix, *Chem. Soc. Rev.* **39**, 1073 (2010).
- [7] K. F. Rinne, S. Gekle, D. J. Bonthuis, and R. R. Netz, *Nano Lett.* **12**, 1780 (2012).
- [8] Q. L. Zhang, W. Z. Jiang, J. Liu, R. D. Miao, and N. Sheng, *Phys. Rev. Lett.* **110**, 254501 (2013).
- [9] U. Zimmerli, P. G. Gonnet, J. H. Walther, and P. Koumoutsakos, *Nano Lett.* **5**, 1017 (2005).
- [10] T. Dumitrica, C. M. Landis, and B. I. Yakobson, *Chem. Phys. Lett.* **360**, 182 (2002).
- [11] R. Garcia-Fandino and M. S. P. Sansom, *Proc. Natl. Acad. Sci. U.S.A.* **109**, 6939 (2012).
- [12] L. H. Yang, V. D. Gordon, D. R. Trinkle, N. W. Schmidt, M. A. Davis, C. DeVries, A. Som, J. E. Cronan, G. N. Tew, and G. C. L. Wong, *Proc. Natl. Acad. Sci. U.S.A.* **105**, 20595 (2008).
- [13] S. Meng, W. L. Wang, P. Maragakis, and E. Kaxiras, *Nano Lett.* **7**, 2312 (2007).
- [14] R. K. Joshi, P. Carbone, F. C. Wang, V. G. Kravets, Y. Su, I. V. Grigorieva, H. A. Wu, A. K. Geim, and R. R. Nair, *Science* **343**, 752 (2014).
- [15] D. Cohen-Tanugi and J. C. Grossman, *Nano Lett.* **12**, 3602 (2012).
- [16] K. Murata, K. Mitsuoka, T. Hirai, T. Walz, P. Agre, J. B. Heymann, A. Engel, and Y. Fujiyoshi, *Nature (London)* **407**, 599 (2000).
- [17] B. L. de Groot and H. Grubmuller, *Science* **294**, 2351 (2001).
- [18] E. Tajkhorshid, P. Nollert, M. O. Jensen, L. J. W. Miercke, J. O'Connell, R. M. Stroud, and K. Schulten, *Science* **296**, 525 (2002).
- [19] A. V. Raghunathan and N. R. Aluru, *Phys. Rev. Lett.* **97**, 024501 (2006).
- [20] A. Kalra, S. Garde, and G. Hummer, *Proc. Natl. Acad. Sci. U.S.A.* **100**, 10175 (2003).
- [21] J. Li, H. M. Li, X. Q. Liang, S. O. Zhang, T. Zhao, D. G. Xia, and Z. Y. Wu, *J. Phys. Chem. A* **113**, 791 (2009).
- [22] C. Y. Lee, W. Choi, J. H. Han, and M. S. Strano, *Science* **329**, 1320 (2010).
- [23] W. Choi, C. Y. Lee, M. H. Ham, S. Shimizu, and M. S. Strano, *J. Am. Chem. Soc.* **133**, 203 (2011).
- [24] W. Choi, Z. W. Ulissi, S. F. E. Shimizu, D. O. Bellisario, M. D. Ellison, and M. S. Strano, *Nat. Commun.* **4**, 2397 (2013).
- [25] B. Corry, *J. Phys. Chem. B* **112**, 1427 (2008).
- [26] C. Song and B. Corry, *J. Phys. Chem. B* **113**, 7642 (2009).
- [27] G. Hummer, J. C. Rasaiah, and J. P. Noworyta, *Nature (London)* **414**, 188 (2001).
- [28] S. Joseph and N. R. Aluru, *Nano Lett.* **8**, 452 (2008).
- [29] M. Majumder, N. Chopra, R. Andrews, and B. J. Hinds, *Nature (London)* **438**, 44 (2005).
- [30] J. K. Holt, H. G. Park, Y. M. Wang, M. Stadermann, A. B. Artyukhin, C. P. Grigoropoulos, A. Noy, and O. Bakajin, *Science* **312**, 1034 (2006).
- [31] J. A. Thomas and A. J. H. McGaughey, *Phys. Rev. Lett.* **102**, 184502 (2009).
- [32] Y.-X. Jia, H.-L. Li, M. Wang, L.-Y. Wu, and Y.-D. Hu, *Sep. Purif. Technol.* **75**, 55 (2010).
- [33] B. Corry, *Energy Environ. Sci.* **4**, 751 (2011).
- [34] Z. E. Hughes, C. J. Shearer, J. Shapter, and J. D. Gale, *J. Phys. Chem. C* **116**, 24943 (2012).
- [35] K. Zhao and H. Wu, *J. Phys. Chem. B* **116**, 13459 (2012).
- [36] W. F. Chan, H. Y. Chen, A. Surapathi, M. G. Taylor, X. H. Hao, E. Marand, and J. K. Johnson, *ACS Nano* **7**, 5308 (2013).
- [37] L. Huang, S. P. Lau, D. G. McCulloch, W. H. Zhong, C. Q. Sun, Y. Q. Fu, and B. K. Tay, *Carbon* **43**, 654 (2005).
- [38] X. S. Li, G. Y. Zhu, J. S. Dordick, and P. M. Ajayan, *Small* **3**, 595 (2007).
- [39] F. Fornasiero, H. G. Park, J. K. Holt, M. Stadermann, C. P. Grigoropoulos, A. Noy, and O. Bakajin, *Proc. Natl. Acad. Sci. U.S.A.* **105**, 17250 (2008).
- [40] Z. W. Ulissi, S. Shimizu, C. Y. Lee, and M. S. Strano, *J. Phys. Chem. Lett.* **2**, 2892 (2011).
- [41] J. C. Ma and D. A. Dougherty, *Chem. Rev.* **97**, 1303 (1997).
- [42] D. A. Dougherty, *Acc. Chem. Res.* **46**, 885 (2013).
- [43] A. S. Mahadevi and G. N. Sastry, *Chem. Rev.* **113**, 2100 (2013).
- [44] M. S. Marshall, R. P. Steele, K. S. Thanthiriwatte, and C. D. Sherrill, *J. Phys. Chem. A* **113**, 13628 (2009).
- [45] H. J. Kulik, E. Schwegler, and G. Galli, *J. Phys. Chem. Lett.* **3**, 2653 (2012).
- [46] B. Song, J. W. Yang, J. J. Zhao, and H. P. Fang, *Energy Environ. Sci.* **4**, 1379 (2011).
- [47] M. Y. Duan, B. Song, G. S. Shi, H. K. Li, G. F. Ji, J. Hu, X. R. Chen, and H. P. Fang, *J. Am. Chem. Soc.* **134**, 12104 (2012).
- [48] G. S. Shi, Z. G. Wang, J. J. Zhao, J. Hu, and H. P. Fang, *Chin. Phys. B* **20**, 068101 (2011).
- [49] G. S. Shi, J. Liu, C. L. Wang, B. Song, Y. S. Tu, J. Hu, and H. P. Fang, *Sci. Rep.* **3**, 3436 (2013).
- [50] G. S. Shi, Y. Shen, J. Liu, C. L. Wang, Y. Wang, B. Song, J. Hu, and H. P. Fang, *Sci. Rep.* **4**, 6793 (2014).
- [51] M. J. Frisch *et al.*, *Gaussian-09, Revision A.01* (Gaussian Inc., Wallingford, CT, 2009).
- [52] See Supplemental Material at <http://link.aps.org/supplemental/10.1103/PhysRevLett.115.164502> for more detailed methods and additional tests, which includes Refs. [53–61].
- [53] L. Verlet, *Phys. Rev.* **159**, 98 (1967).
- [54] S. A. Adelman and J. D. Doll, *J. Chem. Phys.* **64**, 2375 (1976).
- [55] J. P. Ryckaert, G. Ciccotti, and H. J. C. Berendsen, *J. Comput. Phys.* **23**, 327 (1977).
- [56] W. L. Jorgensen, J. Chandrasekhar, J. D. Madura, R. W. Impey, and M. L. Klein, *J. Chem. Phys.* **79**, 926 (1983).
- [57] A. D. Mackerell, J. Wiorcikiewicz-kuczera, and M. Karplus, *J. Am. Chem. Soc.* **117**, 11946 (1995).

- [58] W. Humphrey, A. Dalke, and K. Schulten, *J. Mol. Graphics Modell.* **14**, 33 (1996).
- [59] A. D. MacKerell *et al.*, *J. Phys. Chem. B* **102**, 3586 (1998).
- [60] F. M. Bickelhaupt and E. J. Baerends, *Rev. Comput. Chem.* **15**, 1 (2000).
- [61] G. te Velde, F. M. Bickelhaupt, E. J. Baerends, C. F. Guerra, S. J. A. Van Gisbergen, J. G. Snijders, and T. Ziegler, *J. Comput. Chem.* **22**, 931 (2001).
- [62] J. C. Phillips, R. Braun, W. Wang, J. Gumbart, E. Tajkhorshid, E. Villa, C. Chipot, R. D. Skeel, L. Kalé, and K. Schulten, *J. Comput. Chem.* **26**, 1781 (2005).
- [63] F. L. Hirshfeld, *Theor. Chim. Acta* **44**, 129 (1977).
- [64] C. K. Huang, P. Y. K. Choi, and L. W. Kostiuk, *Phys. Chem. Chem. Phys.* **13**, 20750 (2011).
- [65] G. S. Shi, Y. H. Ding, and H. P. Fang, *J. Comput. Chem.* **33**, 1328 (2012).